Available online at www.sciencedirect.com
ScienceDirect
Polymer 48 (2007) 4837–4848
polymer
www.elsevier.com/locate/polymer

Structure and phase behavior of a disk-necklace polymer: Cyclolinear polymethylsiloxane

Denis V. Anokhin [a], Raluca I. Gearba [a,1], Yuli K. Godovsky [b,2], Sergei N. Magonov [c,3], Natalia N. Makarova [d], Roman I. Ivanov [e], Wim Bras [f], Dimitri A. Ivanov [a,*]

[a] *Institut de Chimie des Surfaces et Interfaces (ICSI), UPR CNRS 9069, 15 rue Jean Starcky, B.P. 2488, 68057 Mulhouse Cedex, France*
[b] *Department of Polymer Materials, Karpov Institute of Physical Chemistry, 10 Vorontsovo Pole, 105064 Moscow, Russia*
[c] *Veeco Metrology Group, 112 Robin Hill Road, Santa Barbara, CA 93117, USA*
[d] *Nesmeyanov Institute of Organoelement Compounds, Russian Academy of Sciences, 28 Vavilov Street, 117813 Moscow, Russia*
[e] *Estonian Nanotechnology Competence Center, Riia Street 142, 51014 Tartu, Estonia*
[f] *Netherlands Organization for Scientific Research (NWO), DUBBLE-CRG/ESRF, B.P. 220, F-38043 Grenoble Cedex, France*

Received 18 March 2007; received in revised form 22 May 2007; accepted 28 May 2007
Available online 13 June 2007

Abstract

The structure and phase transitions of cyclolinear polyorganosiloxane copolymer containing 12-member polysiloxane rings have been studied using synchrotron WAXS, DSC, TEM, variable-temperature AFM and polarized optical microscopy. The primary structure of this polymer can be viewed as a necklace of disk-shaped entities (cyclic groups) connected via flexible linkers.

In the mesomorphic state, the presence of two different LC phases has been derived from the analysis of WAXS fiber diffractograms. The morphology of one of the phases shows a conventional hexagonal packing of LC chains where the chain axes are perpendicular to the plane of the 2D hexagonal lattice. The other one, so-called R-phase, has a vertically oriented rectangular 2D lattice formed by inter-chain correlations between the bulky polysiloxane cycles (disks). To our knowledge, such a disk-necklace mesophase in which the LC lattice is parallel to the backbone direction has not been reported in the literature so far.

Keywords: Mesomorphic polymethylsiloxane; Mesophase-assisted crystallization; Disk-necklace polymer

1. Introduction

Morphology and physical properties of polysiloxanes with new molecular architectures have received significant attention in recent years [1–6]. Much of the interest has been centered on their mesomorphism and polymorphism, in relation to morphology and chemical composition. Among polysiloxanes without mesogenic groups in the chemical structure that exhibit mesomorphism, two groups of macromolecules have attracted particular attention: poly(di-*n*-alkylsiloxane)s and cyclolinear polyorganosiloxanes. Poly(di-*n*-alkylsiloxane)s with ethyl to hexyl side-chains exhibit various crystalline modifications in a wide temperature range. At higher temperatures mesophases, in which extended macromolecules are arranged on a 2D hexagonal lattice without long-range order along the chain direction, are formed. This structure resembles columnar phases formed by a number of liquid crystalline polymers [5] and small molecular weight compounds [cf. for example Refs. [7–9] and references therein]. Morphological characterization with polarized optical microscopy [10–13], electron microscopy [12–14] and atomic force microscopy (AFM) [15–17] has revealed the formation of extended-chain

* Corresponding author. Tel.: +33 389608701; fax: +33 389608799.
E-mail address: dimitri.ivanov@uha.fr (D.A. Ivanov).
[1] Present address: Brookhaven National Laboratory, National Synchrotron Light Source, 75 Brookhaven Avenue, Upton, NY 11973, USA.
[2] Unexpectedly passed away on May 23, 2005.
[3] Present address: Agilent Technologies, 4330 Chandler Blvd, Chandler AZ 85226, USA.

0032-3861/$ - see front matter © 2007 Published by Elsevier Ltd.
doi:10.1016/j.polymer.2007.05.077

lamellar structures in the mesophase. In the case of polydiethylsiloxane (PDES) and polydipropylsiloxane (PDPS) these findings were confirmed by small-angle neutron scattering data and molecular modeling [18]. For most of mesomorphic poly(di-*n*-alkylsiloxane)s spherulites, common morphological features of conventional semicrystalline polymers [19–22], have not been observed in the bulk crystalline state. This indicates that crystal growth is anisotropic and may be dependent on the orientation of the ''parent'' mesophase. Being similar to high-pressure PE [23–25], the morphologies of the crystalline and mesomorphic phases of PDES [1–3,12,17], PDPS [1–3,26,27], and other members of the siloxane family [1–3] allowed to explore in some more detail the formation of extended-chain conformation. A relatively high degree of crystallinity, which is a direct consequence of the mesophase-assisted crystallization, is a common characteristic of many of these polymers [27].

During the last two decades another family of non-mesogenic polysiloxane polymers, cyclolinear polyorganosiloxanes (CLPOS), consisting of linear chains incorporating siloxane cycles of various dimensions bonded either by only oxygen atoms or by flexible spacers, has been developed [1,6,28–30]. The general formula of this class of polysiloxanes is the following:

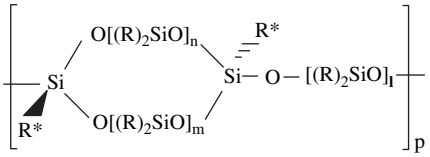

where R, R* are alkyl or aryl substitutes, R = R* or R ≠ R*; $m = 1, 2$; $n = 1, 2$; $l \geq 0$. The number of repeat cycles p in the macromolecule ranges from only a few to several hundred units. The CLPOSs family now consists of about 100 macromolecules, including homopolymers, oligomers, statistical, regular and block copolymers [6,30]. Similar to linear poly(di-*n*-alkylsiloxane)s, as well as to other hybrid inorganic–organic polymers – polyphosphazenes [1,4,5,31–34] and polysilanes [4,35,36], CLPOSs are able to form liquid crystalline (mesomorphic) state. Typical CLPOSs with alkyl substituents and a small number of aryl substituents are rather flexible. However, in spite of their flexibility, the temperature interval of the CLPOS mesophase stability may be surprisingly broad (up to 300°). This is dependent on the cycle molecular weight, the nature of the side-chains and spacers, as well as on the local tacticity in silsesquioxane fragments and the degree of polymerization.

Studies of phase behavior and mesophase structure of the cyclolinear polyorganosiloxanes have shown that 2D-columnar ordering in the mesophase is not a general phenomenon for CLPOSs. The formation of a novel mesophase with 1D-order has been suggested for a series of CLPOSs containing cyclohexasiloxane chain fragments with R* being methyl or phenyl group. The most probable arrangement of the CLPOSs with cyclohexasiloxane chain fragments in the mesomorphic state is layer packing formed by monomolecular layers stacked with a high degree of long-range order [30]. Within the layer, the cyclohexasiloxane fragments are arranged with a strong tendency to lie on their flat sides parallel to the layers. The temperature interval of 1D-mesophase can be modified by varying the chemical structure. Importantly, the interlayer periodicity is mainly dependent on the cyclohexasiloxane thickness, and is rather insensitive to other structural elements of these macromolecules. This conclusion has stimulated investigations of the spreading behavior of these new polysiloxane macromolecules at the air/water interface [37–43]. Similar to the classical amphiphilic polysiloxane – PDMS, the chains with methyl substituents can easily form Langmuir monolayers at the air/water interface. However, in contrast to PDMS, they demonstrate a step-wise collapse during lateral compression, resulting in the formation of stable multilayers at the air/water interface. Such multilayers consisting of up to seven monolayers have been obtained and characterized in situ by Brewster Angle Microscopy, synchrotron X-ray reflectivity and grazing angle X-ray diffraction, as well as ex situ (i.e. after transferring the monolayers and multilayers on solid surfaces) by AFM [40–43]. It was unequivocally demonstrated that the spreading behavior is directly related to the mesophase structure in the bulk.

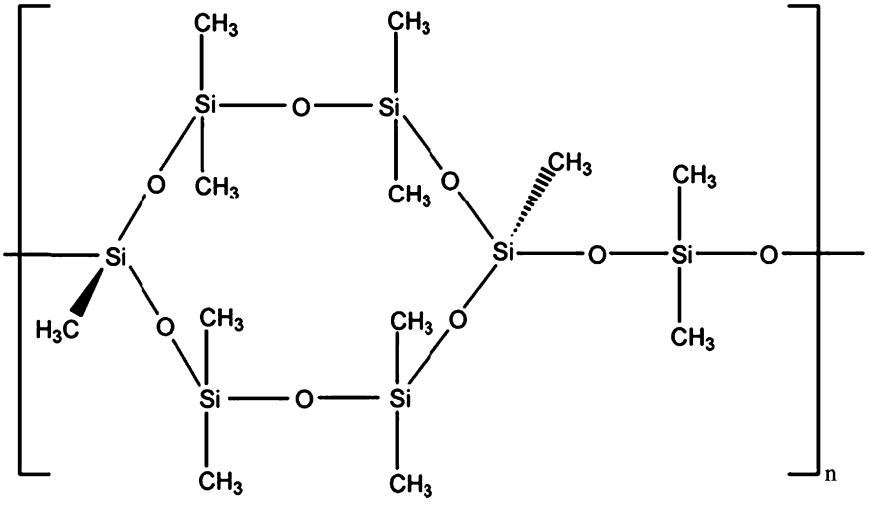

Preliminary characterization of the phase behavior and morphology of cyclolinear polyorganosiloxanes has been carried out and is described elsewhere [28–30]. In the present work we report on a more detailed structural and morphological study of the crystalline and mesomorphic states carried out using a combination of synchrotron X-ray scattering, dilatometry, AFM, and polarized optical microscopy (POM).

2. Experimental

2.1. Materials

The chemical structure of the copolymer sample studied in this work is the following:

The repeating unit of the copolymer is a 12-member ring consisting of six alternating Si and O atoms in a ring. The dimethylsiloxane fragment located outside the ring serves as a linker between the rings in the backbone. The methyl groups connected to the silsesquioxane silicon atoms (i.e., silicon atoms connected to three oxygen atoms in the chain) define the polymer tacticity. They are in the *trans* alternate positions below and above the plane of the ring. The synthesis of these molecules has been described in detail elsewhere [44]. Below, only the main synthesis scheme and molecular characteristics of the monomer and copolymer are given.

The copolymer was synthesized by heterofunctional polycondensation of a corresponding monomer. *trans*-2,8-Dihydroxy-2,4,4,6,6,8,10,10,12,12-decamethylcyclo-hexasiloxane (**I**) was prepared according to the procedure with separation of isomers [45]. The structure of the monomer (**I**) was characterized by X-ray diffraction and ^{1}H NMR [46]. Poly[oxy(decamethylcyclohexasiloxane-2,8-diyl)-dimethylsiloxane]s (CLPMSiC) were prepared according to the following procedure. To 3.59 g (8.0 mmol) of (**I**) and 1.26 g (16.0 mmol) of C_5H_5N in 1.5 ml of dry diethyl ether a solution of 1.03 g (8.0 mmol) of dimethyldichlorosilane in 2.5 ml of dry diethyl ether was added under argon for 1.0 h. Every two days 20 ml diethyl ether was added to the reaction product, and $C_5H_5N\cdot HCI$ was separated; the solution was washed with water and dried under Na_2SO_4, diethyl ether was removed in vacuo. To a benzene solution of 20 ml CLPMSiC was added CH_3OH (16 ml) under stirring. A white precipitate was separated and dried in vacuo (2.85 g, 70.7%). The intrinsic viscosity of the *trans*-copolymer was found to be 0.19 dL/g. ^{29}Si NMR (Bruker spectrometer P-200SY, solution $CCI_4 + C_6D_6$) spectra of the copolymer contained peaks at (δ ppm): −21.90 (Me_2SiO cycle), −22.00 (Me_2SiO linear) and −67.10 ($MeSiO_{1.5}$). The synthesized samples were finally precipitated in toluene solution by alcohol.

The molecular characteristics of the resulting sample are the following: molecular weight of the repeating unit $M_m = 504$ g/mol, average degree of polymerization $x_w = 80$, molecular weight $M_w = 40 \times 10^3$ g/mol.

2.2. Differential scanning calorimetry (DSC)

Phase transitions in CLPMSiC were studied with a Mettler Toledo 822e heat flux DSC equipped with a LN_2 cooling system. The melting temperatures and enthalpies of In and Zn were used as calibrants.

2.3. Dilatometry [47]

Dilatometry measurements were performed with a small (1 cm^3) high-pressure piston-type dilatometer operating in the temperature range from 233 to 523 K. The construction of the dilatometer and the calibration procedure is described elsewhere [48–50]. Some dilatometric experiments for estimation of the linear thermal expansivity of CLPMSiC have been conducted with a temperature-controlled dilatometer DIL 402C (Netzsch, Germany).

2.4. Polarized optical microscopy (POM)

A polarizing microscope (Olympus Provis AX70) coupled to a Linkam heating stage was used for optical texture inspection. The samples were molded between two glass slides.

2.5. Tapping mode AFM (TM-AFM)

For AFM investigations relatively thick (approx. 150 μm) films of CLPMSiC were deposited on a Si surface. The morphology of polymer layers of various thicknesses was studied in the temperature interval from 243 to 323 K, therefore covering the temperature range of the crystalline and mesomorphic states. Etched Si probes (220 μm in length, resonant frequency in the 150–200 kHz range, stiffness ca. 40 N/m) were used. AFM measurements at elevated and sub-ambient temperatures were performed with a thermal and cooling accessory designed by Veeco.

2.6. X-ray diffraction

X-ray diffraction measurements on oriented samples were performed on beamline BM26 at the European Synchrotron Facility in Grenoble (France) using a photon energy of 10 keV. The data were collected in transmission employing high resolution image plates. The temperature was controlled by a Linkam DSC [52] stage operated under a LN_2 flow. The modulus of the scattering vector s ($s = 2\sin\theta/\lambda$, where θ is the Bragg's angle and λ is the wavelength) was calibrated using three diffraction orders of silver behenate. Fibers with 0.7 mm diameter were obtained by extruding the material in the liquid crystalline phase with a home-built mini-extruder. It was found that the material can be well oriented in the mesophase and the orientation is preserved during the subsequent crystallization on cooling.

2.7. Selected-area electron diffraction (SAED)

For SAED measurements the molten samples were deposited on 100 μm carbon-coated mesh grids. A transmission electron microscope was used (TEM, FEI CM200 operated at 120 kV).

3. Results and discussion

3.1. DSC characterization of phase transitions

Heating and cooling scans of CLPMSiC reveal two main transitions (cf. Fig. 1), the derived parameters are listed in Table 1. The transition at 274–280 K recorded on heating is assigned to melting of the CLPMSiC crystalline phase. The high-temperature transition, at 371–379 K, exhibiting a lower enthalpy, corresponds to the isotropization. A more detailed examination of the thermograms shows that both endothermic peaks are doubled. This feature is observed not only during the very first heating of the sample after synthesis but remains during subsequent heating/cooling cycles. The cooling scan displayed in the same figure clearly shows the composite character of the low-temperature transition, which appears in this case as two separate exothermic peaks.

3.2. Dilatometry characterization of phase transitions

The variation of the specific volume as function of temperature is shown in Fig. 2. Phase transitions are easily detectable in the curves by the corresponding density changes. These occur in the temperature intervals close to those determined by DSC (cf. Table 1). By plotting the specific volume versus temperature (Fig. 2) we can estimate the thermal expansion coefficients for the semicrystalline (below 280 K) (α_{cr}), mesomorphic (280–379 K) (α_{meso}) and isotropic state (above 379 K)($\alpha_{isotrop}$): $\alpha_{cr} = 4.7 \times 10^{-4}\ K^{-1}$, $\alpha_{meso} = 6.9 \times 10^{-4}\ K^{-1}$ and $\alpha_{isotrop} = 7.53 \times 10^{-4}\ K^{-1}$. They show a conventional increasing trend, with the largest variation occurring between the crystalline and mesomorphic states. The melting and isotropization transitions are characterized by a considerable specific volume change, typical of first order phase transitions. These volume changes at ambient pressure are $\Delta V_m = 0.046\ cm^3/g$ and $\Delta V_i = 0.015\ cm^3/g$, corresponding to a relative variation of about 4.75% for melting/crystallization and 1.5% for the isotropization/mesophase formation. Similar results were obtained for melting and isotropization of mesomorphic PDES [48–50]. However, for some other mesomorphic polymers such as polyphosphazenes comparable volume changes for melting and isotropization were observed [1].

Table 1
Thermal behavior of CLPMSiC

Temperature ramp	T_m (K)	ΔH_m (J/g)	T_i (K)	ΔH_i (J/g)
Cooling	248/254[a]	−19.3	350	−2.3
Heating	274/280[a]	20.9	371/379[a]	2.5

[a] Two temperatures are given for the peaks, which are doubled (see text for more details).

The results of high-pressure dilatometric measurements are summarized in Fig. 3. Similarly to other crystalline polymers [48,53], the average slope of dT_m/dP is about 0.6 K/MPa, and the pressure dependence of dT_m/dP displays a slightly nonlinear behavior. This is more pronounced for the isotropization transition. The initial slope of dT_i/dP for the isotropization is larger than 1.2 K/MPa, which can be explained by a considerably lower degree of ordering in the mesomorphic state. The pressure dependence of specific volume shows a very important difference for the two phase transitions (cf. the inserts in Fig. 3). On the one hand, the volume change pertinent to melting decreases for approximately 30% with respect to its

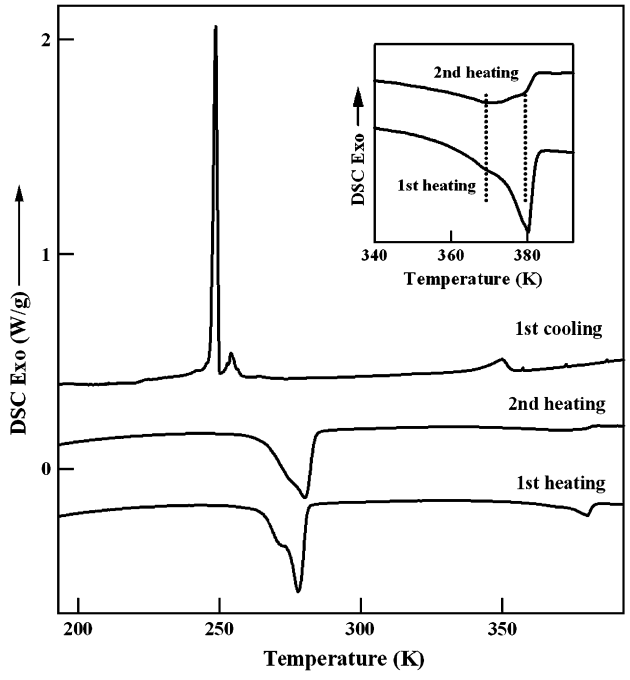

Fig. 1. DSC curves corresponding to heating and cooling ramps of the CLPMSiC sample. The insert gives a closer view of the isotropization peak. The low-temperature transition, occurring in the temperature range of 250–280 K, is assigned to melting of the CLPMSiC crystalline phase. The high-temperature transition, at 350–380 K, exhibiting a lower enthalpy, corresponds to the isotropization. A more detailed examination of the thermograms shows that both transition peaks are doubled.

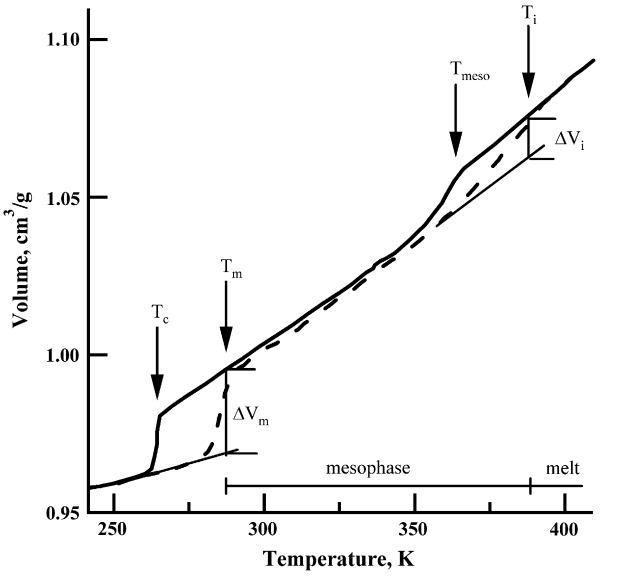

Fig. 2. Specific volume versus temperature for CLPMSiC recorded on heating (full line) and cooling (dashed line). The volume changes associated to the phase transitions are 0.046 and 0.015 cm^3/g for melting/crystallization and the isotropization/mesophase formation, respectively.

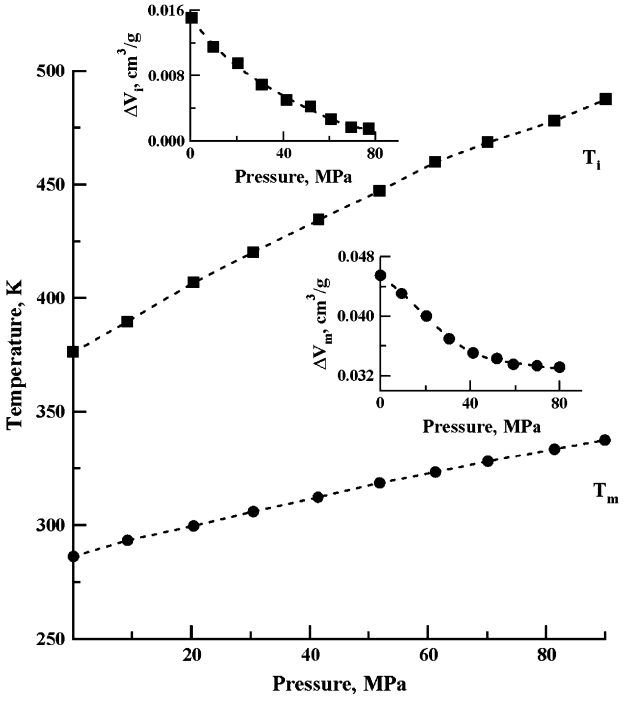

Fig. 3. Phase diagram of the sample. Specific volume versus pressure dependencies for the mesophase (top insert) and crystal phase (bottom insert). The average slope of dT_m/dP is about 0.6 K/MPa; it shows a slight non-linearity. The volume change pertinent to melting (bottom insert) decreases for approximately 30% with respect to its ambient pressure value at a pressure of 40 MPa, and, above this pressure, continues to decrease much slower. The volume change corresponding to the isotropization vanishes above approximately 80 MPa. This indicates that, in these conditions, the specific volumes of the mesophase and the isotropic phase become equal.

ambient pressure value at a pressure of 40 MPa. Above this pressure, it continues to decrease at a much slower pace. On the other hand, the volume change due to the isotropization becomes practically immeasurable above approximately 80 MPa. Similar behavior was previously found for the mesomorphic PDES [50] the isotropization temperature of which starts to decrease with increasing pressure above 160 MPa. This indicates that, in these conditions, the specific volume of the mesophase becomes larger than that of the isotropic phase. In our experiments, the pressure corresponding to the decreasing branch of the isotropization temperature–pressure dependence has not been reached, and therefore the triple point of CLPMSiC remains unknown.

The pressure coefficients of the phase transition temperatures can be expressed from the corresponding specific volume and enthalpy changes by the Clapeyron–Clausius equation:

$$dT_{tr}/dP = T_{tr}\Delta V_{tr}/\Delta H_{tr}$$

where ΔH_{tr} and ΔV_{tr} are the enthalpy and volume changes resulting from the first order phase transition at a temperature T_{tr}. If one takes the initial slopes of dT_{tr}/dP, the enthalpy change accompanying melting reads as: $\Delta H_m = T_m\Delta V_m/(dT_m/dP) = 20 \pm 0.5$ (J/g). This value is in good agreement with results from DSC measurements (cf. Table 1). However, the heat of isotropization ΔH_i is given by $\Delta H_i = T_i\Delta V_i/(dT_i/dP) = 5.0 \pm 0.2$ (J/g), which is approximately twice the corresponding DSC value. To explain this discrepancy, it has to be noted that the heat of isotropization was found to be quite sensitive to the sample thermal history. ΔH_i significantly increases upon a long-term annealing at room temperature, whereby the ratio of the components of the doubled peak in the DSC traces changes (cf. for example the first heating in Fig. 1). The deviation from the Clapeyron–Clausius equation is an indication of the complexity of the phase diagram of CLPMSiC in which more than one mesophase is present. This issue will be discussed in more detail further on.

3.3. POM observations of CLPMSiC morphology in the mesomorphic state

Polarized light microscopy shows that when cooling the sample from the isotropic phase a birefringent texture appears due to the development of the mesophase at 368 K (see Fig. 4). One can see the growth of birefringent needle-like features that can be assigned to the mesomorphic lamellae oriented edge-on. The length and width of the lamellae are approximately 30 and 2 μm, respectively. This texture is typical for a number of polysiloxanes forming columnar mesophases [1], as well as for other mesomorphic polymers forming hexagonal mesophases such as 1,4-*trans*-polybutadiene [54] or PE at high pressure [20].

3.4. TM-AFM observation of CLPMSiC morphology in mesomorphic and crystalline states

The morphology after cooling the sample from the isotropic state was also studied by AFM. Fig. 5A shows relatively ordered stacks of crystalline lamellae, with an average thickness of 180 nm. This thickness significantly exceeds the contour length of one chain (73 nm), which means that these are not simply extended-chain lamellae. In higher resolution images (Fig. 5B, C) measured at ambient temperature, the lamellae reveal a fine structure consisting of bright and dark stripes running at a small angle with respect to the lamellar edge. This fine structure is invariably present in both, the crystalline as well as the LC states. The contrast observed in phase images indicates that the regions corresponding to both types of stripes differ in their physical properties. To quantify the structural parameters, we have performed analysis of the images using the SAXS-type one-dimensional correlation and interface distribution functions (IDF) described elsewhere [55,56]. A typical IDF shown in Fig. 5D displays a relatively broad maximum with the most probable value at about 15 nm and a long period (first minimum) of 33 nm. The distance of 15 nm corresponds to the characteristic thickness of a single stripe. Thus, despite the organization in very thick lamellae, the structure of CLPMSiC remains heterogeneous at the scale characteristic of conventional semicrystalline polymers. Based on the long period, one may suggest that some of the chains are folded once.

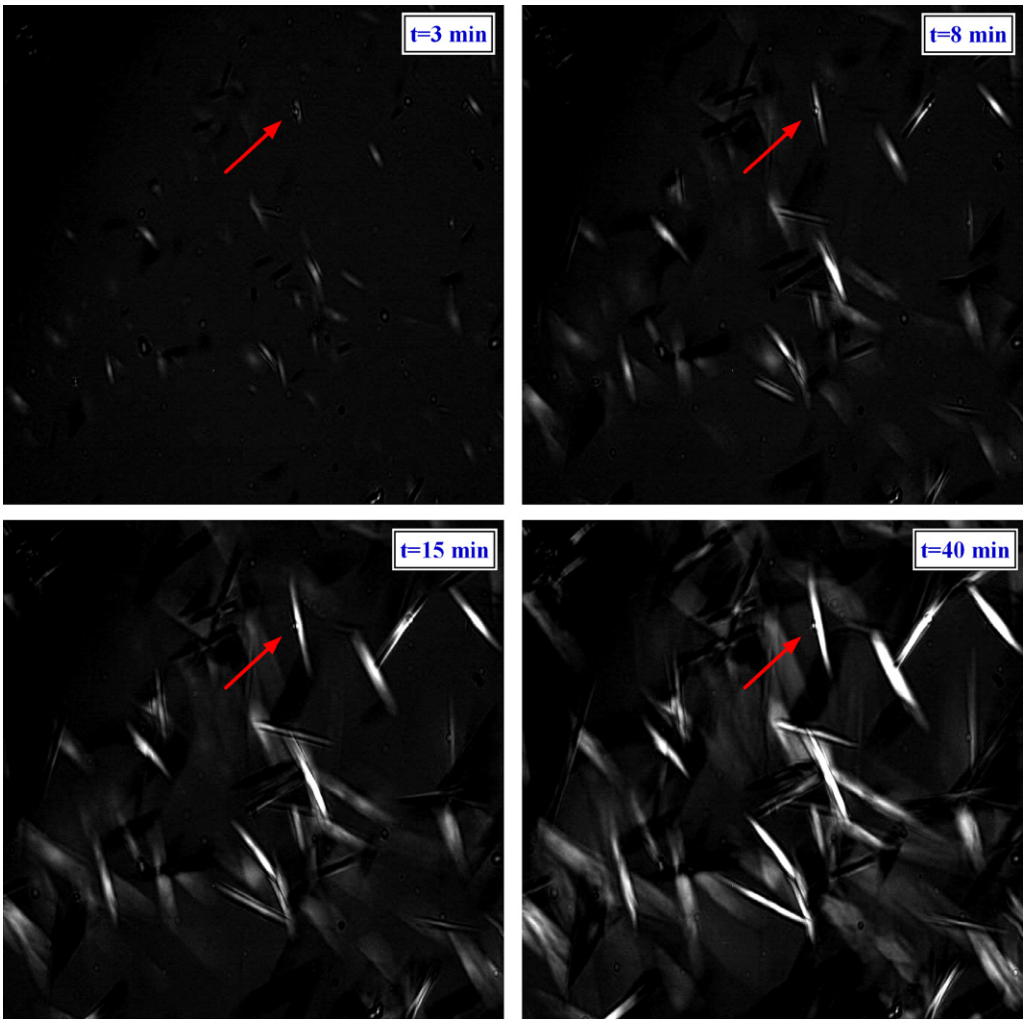

Fig. 4. Optical textures measured in polarized light after different annealing times at 368 K. The sample was initially heated to the isotropic state and then rapidly brought to the annealing temperature. The arrows in the micrographs point at a single growing mesomorphic lamella. The size of the images is 865 × 650 μm^2.

3.5. Selected-area electron diffraction of CLPMSiC in the mesophase

Electron diffraction patterns of a thin film of CLPMSiC show a characteristic 6-fold symmetry pattern (see Fig. 6). It can be assigned to a homeotropically oriented mono-domain, with a hexagonal unit cell having $a = 9.53$ Å. We were not able to record a diffraction pattern corresponding to the in-plane chain orientation. One of the possible reasons for that could be a significant thickness of the edge-oriented lamellae. Indeed, from the AFM image shown in Fig. 5A the height of the lamellar features exceeds 350 nm, which is prohibitive for TEM observations.

3.6. X-ray structural analysis of CLPMSiC in the mesomorphic and crystalline states

X-ray fiber diffractograms show that CLPMSiC can be easily oriented in the mesophase by extrusion (Fig. 7B) and the orientation is preserved during subsequent crystallization on cooling (Fig. 7A). A 2D X-ray pattern measured at 223 K corresponding to the crystalline phase resulting from the crystallization of the oriented mesophase is given in Fig. 7A. It displays 32 sharp reflections approximately distributed over five layer lines (Table 2). Note the presence of five diffraction orders in the chain direction. The peak positions can be indexed to a triclinic unit cell with parameters $a = 8.87$ Å, $b = 17.12$ Å, $c = 18.92$ Å (fiber repeat), $\alpha = 90°$, $\beta = 82.2°$ and $\gamma = 88.3°$. By assuming that the unit cell accommodates two chains, the crystalline phase density of 1.01 g/cm^3 can be found. The degree of crystallinity calculated from the diffractogram is very high (0.83), which is typical for the mesophase-assisted crystallization of main-chain LC polymers [27].

X-ray pattern recorded in the mesophase at room temperature (Fig. 7B) displays three equatorial reflections located at 8.40, 4.76 and 4.18 Å with relative spacings given by the ratio: 1:$\sqrt{3}$:2 (Table 3). This indicates a two-dimensional hexagonal lattice, which is formed by the chain axes. The corresponding lattice parameter $a_h = 9.66$ Å. Such assignment is in agreement with the electron diffraction results described above. However, in addition to equatorial peaks, the X-ray pattern shows sharp off-meridional peaks located on the first and

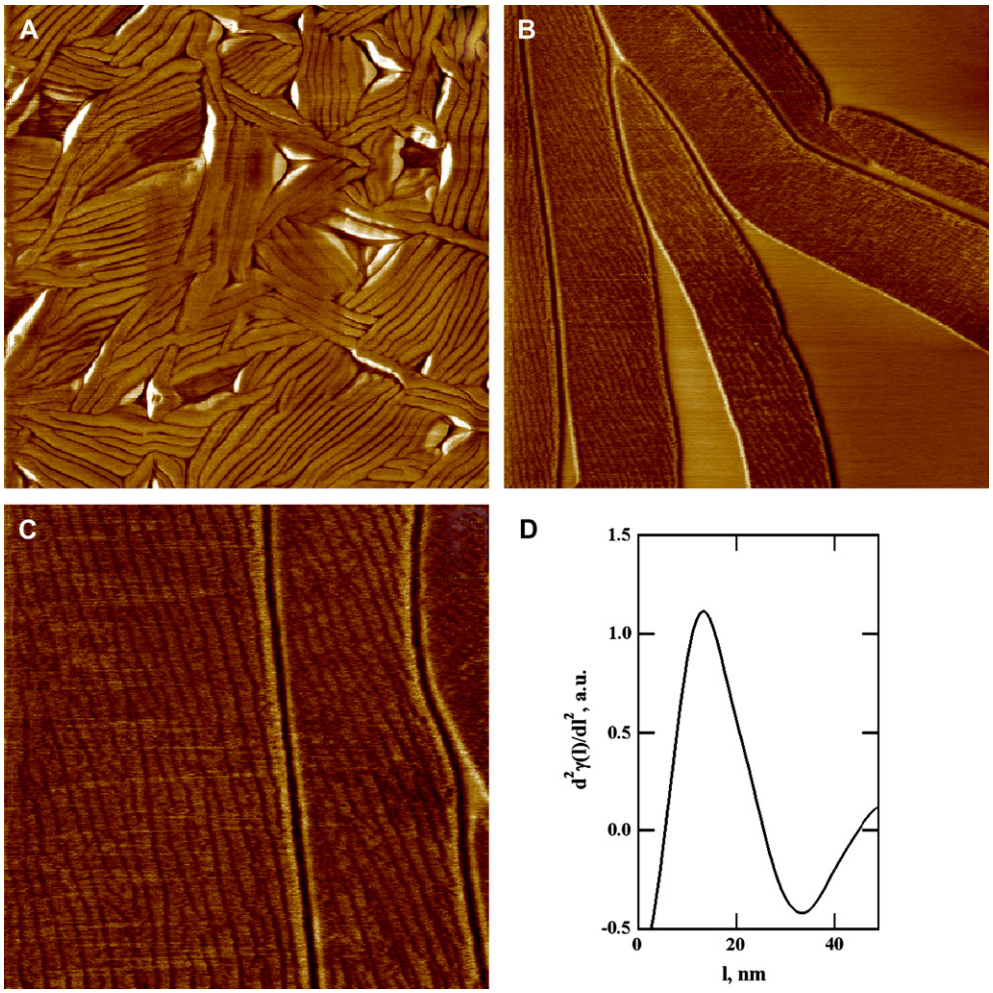

Fig. 5. Taping mode AFM phase images of the CLPMSiC sample measured on different scales: 10×10 μm^2 at 243 K (A), 2×2 μm^2 at 323 K (B), 1×1 μm^2 at 323 K (A-C). (D) SAXS-type interface distribution function calculated for image in (C). The thickness of the crystalline lamellae (image in (A)) significantly exceeds the contour length of one chain (73 nm), which means that these are not simply extended-chain lamellae. In addition, the lamellae reveal a fine structure (B, C) consisting of bright and dark stripes. The characteristic thickness of a single stripe evaluated from the IDF (D) is about 15 nm.

second layer lines. The strongest off-meridional peak on the first layer line has a spacing of 8.04 Å. It is undoubtedly the most remarkable structural feature of the CLPMSiC mesophase. Note that X-ray mesophase patterns of a similar polymer, PDES, do not display such peaks [57]. Generally, the presence of sharp off-meridional peaks is an indication that the structure is a 3D crystal. However, that would be at variance with the observations of the pasty appearance of the material, which is an indication of the liquid crystalline character of CLPMSiC at room temperature.

One could also suggest that the presence of the off-meridional peaks is due to incomplete melting of the CLPMSiC crystalline phase. However, the structure of CLPMSiC at room temperature is very different from that in the crystalline phase: for example, the described off-meridional peaks are absent in the X-ray pattern of the crystal (cf. Fig. 7A and Table 2). Therefore one can completely rule out the possibility that this feature of the room temperature X-ray pattern is due to the remaining crystals.

Interestingly, the equatorial peaks at $s = 0.119$ Å^{-1}, together with the off-meridional peaks, form a six-spot pattern with an almost hexagonal symmetry. In the following, this quasi-hexagonal rectangular centered structure will be denoted as the R-phase. Different possibilities have been considered in order to index the mesophase diffraction pattern to a single structure. However, it appears to be a hard task because of the incompatibility of the hexagonal chain axes packing and the quasi-hexagonal structure in the plane parallel to the chains. The simplest argument, which shows the impossibility to build such a single structure, is the following. On the one hand, the vertical and horizontal dimensions of the structural building block (monomer) are close, as can be concluded from the comparison of equatorial versus meridianal spacings. On the other hand, the presence of the quasi-hexagonal packing in the chain direction implies that some of the chains are shifted vertically by half of the fiber repeat. Therefore, in the plane perpendicular to the chain axes, the distances between the chains cannot be all equal due to a vertical shift

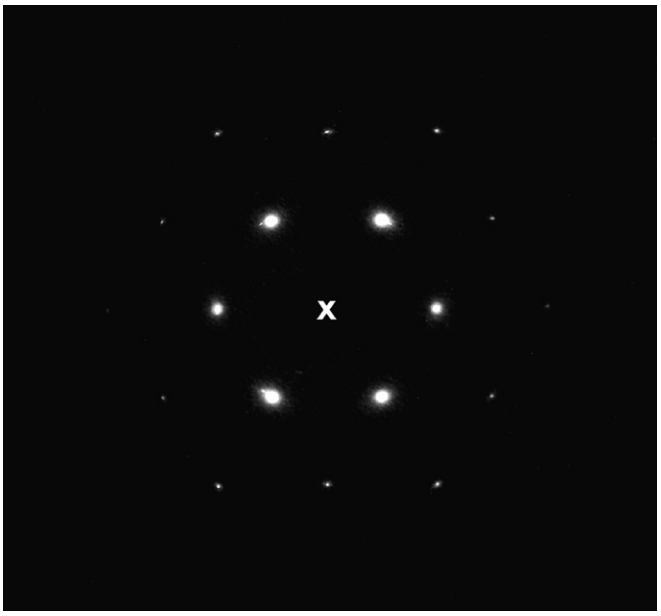

Fig. 6. Electron diffraction pattern of a thin CLPMSiC film deposited on a carbon-coated TEM grid. It can be assigned to a homeotropically oriented mono-domain, with a hexagonal unit cell having $a = 9.53$ Å.

of some of the chains with respect to some others. Therefore, the two lattices, i.e. the hexagonal horizontal and quasi-hexagonal vertical, are incompatible. We thus concluded that at least one equatorial peak and all the non-equatorial peaks are pertinent to two different structures.

Note that, when performed separately, the indexation of both structures does not pose problems (Table 3). Thus the R-phase with parameters $a = 16.76$ and $b = 9.10$ Å (fiber repeat) can account for all the observed off-meridional reflections such as the strongest 11 as well as weaker 31 (4.76 Å) and 22 (4.05 Å) peaks (cf. Table 3). The presence of intense horizontal streaks located on the first and second layer lines

Table 2
X-ray fiber diffraction data measured at 223 K

h	k	l	d_{exp} (Å)	d_{calc} (Å)
1	0	0	8.74	8.79
1	1	0	7.94	7.91
1	2	0	6.25	6.22
2	0	0	4.49	4.39
2	2	0	3.99	3.95
0	0	1	18.69	18.74
1	0	1	8.4	8.40
1	1	1	7.58	7.62
1	2	1	6.12	6.07
1	−2	1	5.78	5.92
2	0	1	4.46	4.41
2	2	1	3.85	3.97
0	0	2	9.37	9.37
1	0	2	6.87	6.89
1	1	2	6.43	6.44
1	2	2	5.44	5.42
2	0	2	4.19	4.20
0	0	3	6.27	6.25
1	0	3	5.45	5.45
0	2	3	5.09	5.04
1	2	3	4.79	4.63
1	−2	3	4.65	4.57
2	0	3	3.86	3.85
0	0	4	4.72	4.69
1	0	4	4.41	4.39
1	2	4	3.94	3.92
1	−2	4	3.61	3.89
2	0	4	3.47	3.45
0	0	5	3.79	3.75
2	0	5	3.14	3.06
0	0	6	3.18	3.12
1	0	6	3.14	3.08

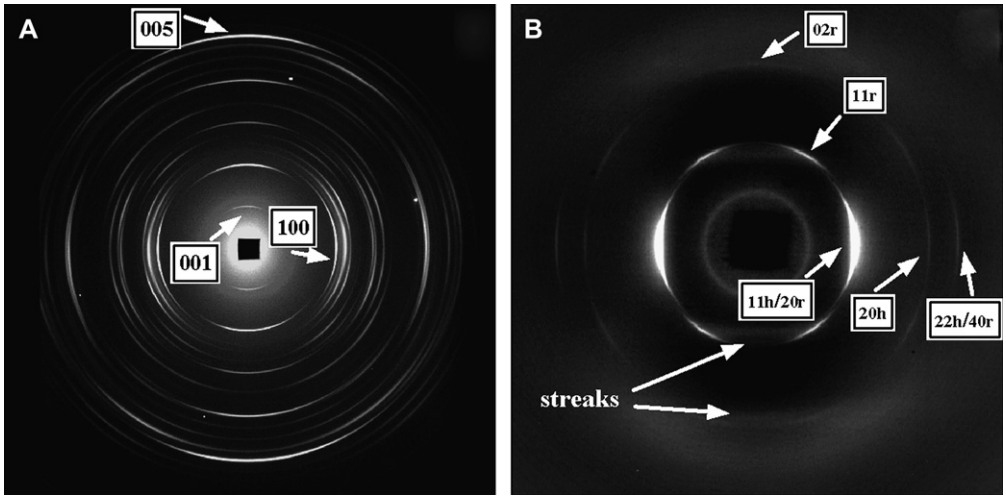

Fig. 7. 2D X-ray diffraction pattern recorded for crystal phase at 223 K (A) and in the mesophase at ambient temperature (B). The peak positions of the crystalline lattice can be indexed to a triclinic unit cell with parameters $a = 8.87$ Å, $b = 17.12$ Å, $c = 18.92$ Å (fiber repeat), $\alpha = 90°$, $\beta = 82.2°$ and $\gamma = 88.3°$. The diffraction pattern of the mesophase cannot be indexed to a single structure. Therefore we suppose that, in addition to a conventional hexagonal mesophase, there exists another mesophase (termed the R-phase), which is responsible for the appearance of the off-meridional peaks.

Table 3
X-ray fiber diffraction data measured at 293 K

Phase[a]	*h*	*k*	d_{exp} (Å)	d_{calc} (Å)
h	1	1	8.40	8.38
r	2	0		
h	2	0	4.86	4.83
h	2	2	4.18	4.19
r	4	0		
r	1	1	8.04	8.00
r	3	1	4.76	4.76
r	0	2	4.59	4.55
r	2	2	4.05	4.00

[a] h stands for the hexagonal and r for rectangular R-mesophase.

close to the meridional direction indicates that the structure of the R-phase exhibits defects in the fiber axis direction, i.e. the chains in the 2D lattice of the R-phase are translationally disordered along the chain direction. We are not aware of any LC phase with a similar 2D lattice oriented along the chain axis.

Following the referee's comments, we have analyzed the X-ray patterns of the CLPMSiC mesophase with more scrutiny to check the hypothesis about the co-existence of two different mesophases. Fig. 8 shows one-dimensional WAXS profiles measured upon a long-time annealing of a CLPMSiC fiber at room temperature (left) and shortly after cooling it to the crystalline phase and heating back to room temperature (right). Decomposition of the intensity into two sharp peaks (r_{20}/h_{11} and r_{11}) and one broad peak (streak) allows comparing the intensities of the peaks, which are supposedly pertinent to two different mesophases. It was found that, upon crystallization and melting, the intensity of r_{11} with respect to the r_{20}/h_{11} peak decreases from 1:15.1 to 1:33.1. This confirms the hypothesis about the co-existence of the two mesophases.

3.7. Polymorphism of disk-necklace structures

The two LC structures described above are schematically depicted in Fig. 9. The first one shown in the top panel corresponds to the usual columnar mesophase formed by polymer chains, i.e. when the upright standing columns are arranged on a 2D hexagonal lattice. The bottom panel shows the second structure, i.e. the novel R-phase, in which the liquid crystalline order is built up in the vertical plane, along the chain axes. In this case, the neighboring chains are correlated with each other not only via regular positioning of the backbones but also due to the inter-chain register of the polysiloxane cycles. It is clear that the building blocks for both structures are the bulky polysiloxane cycles present in the main chain. At the mesoscale level, the chains can be viewed as necklaces of nanometer-sized disks, and the LC structures are obtained by the assembly of these disk-necklaces.

In the usual columnar phase, the cycles (disks) pertinent to one chain are stacked in the vertical direction, whereas in the second case the cycles pertinent to different chains are stacked in the direction perpendicular to the chain axis. The driving force in both cases could be segregation between the siloxane cores and aliphatic periphery of the cycles, which can occur

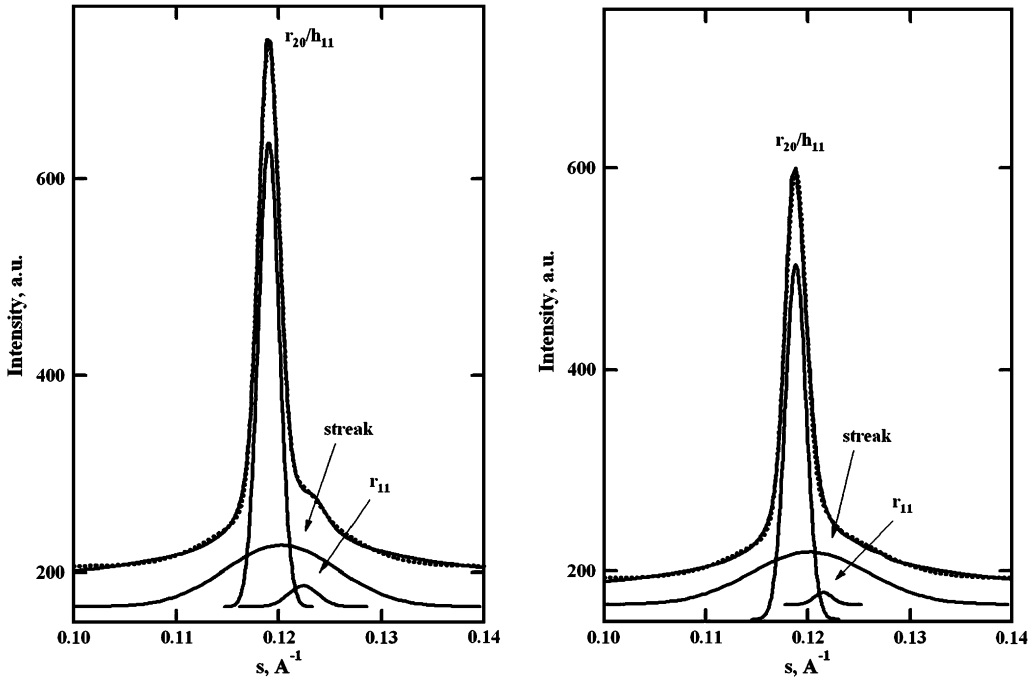

Fig. 8. 1D WAXS profiles calculated from 2D patterns for a CLPMSiC fiber annealed for three weeks at room temperature (left) and the same fiber measured shortly after cooling to 223 K and heating back to room temperature (right). Decomposition of a composite peak located at approximately 0.12 $Å^{-1}$ allows to compare the relative intensities of the r_{20}/h_{11} and r_{11} peaks. The dotted lines are fits of the measured intensity with a sum of three Gaussians. The ratio between the surfaces under these peaks changes from 15.1 (left) to 33.1 (right). This indicates that the peaks are pertinent to two different mesophases, which are simultaneously present in the sample.

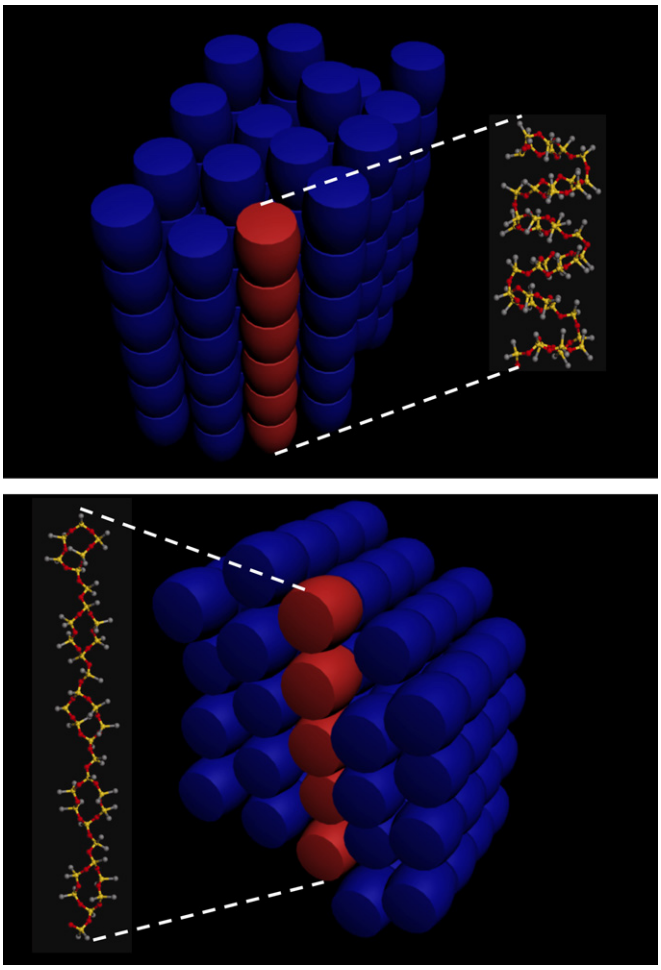

Fig. 9. Schematic representation of the structure of two coexisting hexagonal mesophases of CLPMSiC. The 2D hexagonal lattice is formed either perpendicular to the main-chain axis, as in the conventional case (top panel), or in a plane parallel to the chains (bottom). The observed polymorphism can be accounted for, on the one hand, by the presence of nanometer size disk-shaped entities in the chain structure (siloxane cycles), and, on the other hand, by the flexibility of the spacers connecting the cycles.

via inter- and intra-chain stacking. Accordingly, the possible chain conformations compatible with the two phases are given in Fig. 9. It is noteworthy that the conformation of the polysiloxane cycle can be variable due to the flexibility of the PDMS chain [58]. The conformation lability of the cycle and flexibility of the linkers connecting the cycles are thus likely to account for the possibility of CLPMSiC to self-organize in these two different ways.

Generally, the liquid character of the phases (i.e. the large-scale molecular motion of the chains) should correspond to reduced spatial correlations in some directions [cf. Ref. [59] and references therein]. For the R-phase, the inter-chain correlations should be reduced in the direction perpendicular to the rectangular lattice, i.e. along the **c** vector. Therefore, we believe that in this phase the interactions between CLPMSiC chains belonging to different **ab** layers are much weaker than interactions between chains inside the same layer. Note that the equatorial peak corresponding to the interlayer distance coincides with the 110 reflex of the hexagonal lattice, i.e. the diameter and thickness of the polysiloxane cycle are close. The chain mobility can then be explained by free sliding of the layers with respect to each other. This picture qualitatively corroborates previous observations of layer-like structures made on Langmuir films of similar polymers [37–43].

Despite the structural differences between the two LC phases, their thermal properties are likely to be quite similar. First, from the DSC results shown above, the clearing transitions of the phases are close. Second, based on diffraction patterns taken at different temperatures, we found that the linear thermal expansion coefficients of both structures are equal, $3.3 \times 10^{-4}\ K^{-1}$, which is in agreement to the findings from dilatometry. Therefore the phases coexist over the whole temperature range, and are difficult to isolate them experimentally. However, as we have shown, there are indications that the R-phase is thermodynamically stable, and can be formed from the other, hexagonal, phase upon long-term annealing in the LC state. Importantly, despite the presence of two different mesophases, the crystallization results in the formation of only one orientation of the crystalline phase. The conformational transitions accompanying crystallization should therefore be different for the two mesophases. A small difference in the crystallization temperatures can be suggested from the DSC cooling trace, as shown in Fig. 1.

4. Summary and conclusions

The structure and phase transitions of cyclolinear CLPMSiC copolymer containing 12-member polysiloxane rings have been studied by X-ray diffraction, as well as by DSC, TEM, AFM and polarized optical microscopy. The primary structure of this polymer can be viewed as a necklace of disk-shaped entities (cyclic groups) connected via flexible linkers.

In the mesomorphic state, the presence of two different liquid crystalline phases has been derived from the analysis of WAXS fiber diffractograms. One of the phases corresponds to a conventional hexagonal packing of LC chains where the chain axes are perpendicular to the plane of the 2D hexagonal lattice. The other one, so-called R-phase, has a vertically oriented rectangular 2D lattice formed by inter-chain correlations between the bulky polysiloxane cycles. We suggest that the liquid character of the R-phase is accounted for by weaker interactions between the ab layers (the fiber repeat is in the **b**-direction), which allow sliding of the layers with respect to each other and thereby provide the macroscopic chain mobility. The morphology of this mesophase is rather unique and to our knowledge there are no other LC systems which exhibit a similar phase. The supermolecular organization of CLPMSiC is thus closely related to its disk-necklace structure composed of conformationally labile soft bulky groups. The ‘‘softness’’ of the disks capable of self-assembly in two different directions and flexibility of the thread (linkers connecting the cycles) are thought of being mainly responsible for the observed polymorphism of CLPMSiC.

The organization of the mesophases on the nanometer to micrometer scale was investigated by AFM. It is shown that the CLPMSiC chains organize in lamellae with a thickness of about 180 nm. This thickness significantly exceeds the contour length of one chain, similar to the morphology formed by crystallizing HDPE under elevated pressures [24]. The lamellae do not simply contain extended chains but can be organized in a super-chain structure, probably comprising both extended and folded chains. Additionally, a fine intra-lamellar structure was observed, with a characteristic size of about 15 nm. This structure is present in both crystalline and LC states and indicates that the organization of CLPMSiC is heterogeneous at this scale. The presence of such structure implies spatial segregation of chain folds and chain ends in less ordered regions.

The process of crystallization was studied using WAXS. This technique reveals typical features of the mesophase-assisted crystallization during which the crystalline growth occurs anisotropically, using the preordered state of the chains in the mesophase. During crystallization, the chain orientation is preserved and the degree of crystallinity approaches the values typical of PE single crystal mats [60]. On the lamellar scale, the crystallization does not perturb the lamellar structure formed in the mesophase. Therefore the crystallization process in this case is mainly operational on the sub-molecular scale.

Acknowledgements

D.A.I. acknowledges financial support from the ATIP project (CNRS, France) and from the European Community's 'Marie-Curie Actions' under contract MRTN-CT-2004-504052 [POLYFILM]. R.I.G. is a postdoctoral fellow of the Centre National de la Recherche Scientifique (CNRS) of France. This work was financially supported by Russian Foundation for Basic Research (grant No 02-03-32199). We acknowledge the European Synchrotron Facility and NWO/FWO for provision of synchrotron radiation facilities. We thank N. Vilayphiou and F. Meneau for assistance in using the BM26B beamline.

References

[1] Godovsky YK, Papkov VS. Adv Polym Sci 1989;88:129.
[2] Molenberg A, Möller M, Sautter E. Prog Polym Sci 1997;22:1133.
[3] Wunderlich B, Grebovich J. Adv Polym Sci 1984;60/61:1.
[4] Wunderlich B, Möller M, Grebovich J, Baur H. Adv Polym Sci 1988;87:1.
[5] Ungar G. Polymer 1993;34:2050.
[6] Makarova NN, Godovsky YK. Prog Polym Sci 1997;22:1001.
[7] Gearba RI, Lehmann M, Levin J, Ivanov DA, Koch MHJ, Baberá J, et al. Adv Mater 2003;15:1614.
[8] Gearba RI, Bondar AI, Lehmann M, Goderis B, Bras W, Koch MHJ, et al. Adv Mater 2005;17:671.
[9] Gearba RI, Bondar AI, Goderis B, Bras W, Ivanov DA. Chem Mater 2005;17:2825.
[10] Papkov VS, Svistunov VS, Godovsky YK, Zhdanov AA. J Polym Sci Polym Phys Ed 1987;25:1859.
[11] Out G. Ph.D. dissertation, University of Twente, Enschede, The Netherlands; 1994.
[12] Molenberg A, Möller M. Macromolecules 1997;30:8332.
[13] Molenberg A. Ph.D. thesis, University of Ulm, Germany; 1997.
[14] Obolonkova EV, Papkov VS. Vysokomol Soedin 1990;B31:691.
[15] Magonov SN, Elings V, Papkov VS. Polymer 1997;38:297.
[16] Magonov SN, Godovsky YK. Am Lab 1998;30:15.
[17] Godovsky YK, Papkov VS, Magonov SN. Macromolecules 2001;34:976.
[18] Schlottke H. Ph.D. thesis, University of Mainz, Germany; 1995.
[19] Wunderlich B. Macromolecular physics, vol. 1. New York: Academic Press; 1973.
[20] Bassett DC. Principles of polymer morphology. Cambridge, England: Cambridge University Press; 1981.
[21] Barham P. In: Cahn W, Haasen P, Kramer EJ, Thomas EL, editors. Crystallization and morphology of semicrystalline polymers. Materials science and technology, vol. 12. New York: VCH Publishers; 1993.
[22] Bassett DC. In: Keller A, Warner M, Windle AH, editors. Self-order and form in polymeric materials. London: Chapman & Hall; 1995. p. 27–41.
[23] Bassett DC, Turner B. Philos Mag 1974;29:92.
[24] Bassett DC. The crystallization of polyethylenes at high pressures. In: Bassett DC, editor. Developments in crystalline polymers. London, New Jersey: Applied Science; 1982. p. 115–51.
[25] Keller A, Hikosaka M, Rastogi S, Toda A, Barham PJ, Goldbeck-Wood G. In: Keller A, Warner M, Windle AH, editors. Self-order and form in polymeric materials. London: Chapman & Hall; 1995. p. 1–15.
[26] Gearba RI, Dubreuil N, Anokhin DV, Godovsky YK, Ruan JJ, Thierry A, et al. Macromolecules 2006;39:978.
[27] Gearba RI, Anokhin DV, Bondar AI, Godovsky YK, Papkov VS, Makarova NN, et al. Macromolecules 2006;39:988.
[28] Godovsky YK, Makarova NN, Kuzmin NN. Makromol Chem Macromol Symp 1989;26:91.
[29] Godovsky YK, Makarova NN. In: Keller A, Warner M, Windle AH, editors. Self-order and form in polymeric materials. London: Chapman & Hall; 1995. p. 43–55.
[30] Godovsky YK, Makarova NN, Matukhina EV. Mesophase behavior and structure of mesophases in cyclolinear polyorganosiloxanes. In: Clarson S, Fitzgerald JJ, Owen MJ, Smith SD, editors. Silicones and silicone modified materials. ACS symposium series, vol. 729. Washington, D.C.: American Chemical Society; 2000. p. 98–115.
[31] Desper CR, Schneider NS. Macromolecules 1976;9:424.
[32] Schneider NS, Desper CR, Birs JJ. In: Blumstein A, editor. Liquid crystalline order in polymers. New York: Academic Press; 1978.
[33] Magill JH. J Inorg Organomet Polym 1992;2:213.
[34] Papkov VS, Il'ina MN, Zhukov VP, Tsvankin DY, Tur DR. Macromolecules 1992;25:2033.
[35] Weber P, Guillon D, Scoulious A, Miller RD. J Phys (Paris) 1989;50:793.
[36] Schilling FC, Bovey FA, Lovinger AJ, Ziegler JM. In: Ziegler JM, Fearon FMG, editors. Silicon based polymer science. Advances in chemistry, vol. 224. Washington, D.C.: ACS; 1990.
[37] Fang J, Dennin M, Knobler CM, Godovsky YK, Makarova NN, Yokoyama H. J Phys Chem B 1997;101:3147.
[38] Sautter E, Belousov SI, Pechhold W, Makarova NN, Godovsky YK. Polym Sci 1996;A38:39.
[39] Buzin AI, Sautter E, Godovsky YK, Makarova NN, Pechhold W. Colloid Polym Sci 1998;276:1078.
[40] Buzin AI, Godovsky YK, Makarova NN, Fang J, Wang X, Knobler CM. J Phys Chem B 1999;103:11372.
[41] Jensen TR, Kjaer K, Brezesinski G, Ruiz-Garcia J, Möhwald H, Makarova NN, et al. Macromolecules 2003;36:7236.
[42] Godovsky YK, Brezesinski G, Möhwald H, Jensen TR, Kjaer K, Makarova NN. Macromolecules 2004;37:4872.
[43] Godovsky YK, Belousov SI, Makarova NN, Brezesinski G, Möhwald H, Jensen TR, et al. Nonlinear optics and quantum optics, 31; 2004. p. 31.
[44] Makarova NN, Astapova TV, Godovsky YK, Matukhina EV, Lavrukhin BD, Yakubovich. Russ Polym Sci 1993;A35:190.
[45] Makarova NN, Petrova IM, Godovsky YK, Lavrukhin BD, Zhdanov AA. Dokl Akad Nauk SSSR 1983;269:1369.
[46] Furmanova NG, Andrianov VI, Makarova NN. J Struct Chem 1987;28:256.

[47] The dilatometric results presented in this paper were obtained in the frame of scientific cooperation of Department of Polymer Materials, Karpov Institute of Physical Chemistry, Moscow (Y.K. Godovsky) and Department of Applied Physics, Ulm University, Germany (Prof. Dr. W. Pechhold, Dr. E. Sautter).
[48] Dollhopf W, Barry S, Strauss MJ. In: Hochheimer HD, Etter RD, editors. Frontiers of high pressure research. New York: Plenum Press; 1991. p. 25.
[49] Pechhold W, Schwarzenberger P. In: Hochheimer HD, Etter RD, editors. Frontiers of high pressure research. New York: Plenum Press; 1991. p. 57.
[50] Reck T, Sautter E, Dollhopf W, Pechhold W. Rev Sci Instrum 1998;69:1823.
[52] Bras W, Derbyshire GE, Devine A, Clark SM, Cooke J, Komnschek BE, et al. J Appl Crystallogr 1995;28:26.
[53] Privalko VP. Molecular structure and properties of polymers [in Russian]. Leningrad: Khimiya; 1986. p. 191.
[54] Rastogi S, Ungar G. Macromolecules 1992;25:1445.
[55] Basire C, Ivanov DA. Phys Rev Lett 2000;85:5587.
[56] Ivanov DA, Amalou Z, Magonov SN. Macromolecules 2001;34:8944.
[57] Tsvankin DY, Papkov VS, Zhukov VP, Godovsky YK, Svistunov VS, Zhdanov AA. J Polym Sci 1985;23:1043.
[58] Flory PJ. Statistical mechanics of chain molecules. New York: Interscience; 1969.
[59] Auriemma F, De Rosa C, Corradini P. Adv Polym Sci 2005; 181:1.
[60] Hocquet S, Dosière M, Thierry A, Lotz B, Koch MHJ, Dubreuil N, et al. Macromolecules 2003;36:8376.